line.[6,7,10] Since the conductivity of polyaniline arise from anion doping into it, BF_4^- also must be supplied as the dopant where the electropolymerization takes place. When the degree of dissociation of ATFB is small, both anilinium ion and BF_4^- would be supplied to the site where the electropolymerization of aniline takes place. In our case, it seems that the small degree of dissociation of ATFB in MeCN might effect the electropolymerization process to prepare polyaniline which is better for battery use than that of polyaniline prepared in PC or GBL. In addition, the electropolymerization current density influences the discharge and charge characteristics of polyaniline. Polyaniline prepared in MeCN containing 1.0 mol dm^{-3} ATFB at 0.01 mA cm^{-2} had the largest discharge capacity and the smallest effect of the kinetics at 0.1 mA cm^{-2} as shown in Fig. 5. This may be because polyaniline prepared in MeCN containing 1.0 mol dm^{-3} ATFB at 0.1 or 0.01 mA cm^{-2} has a fine fibrous structure which has very large surface area (Fig. 2, Fig. 6).

Acknowledgments

This study was supported by the Grant-in-Aid for Scientific Research from the Ministry of Education, Science and Culture of Japanese Government (No. 03453086).

Manuscript submitted July 15, 1994; revised manuscript received May 31, 1995.

Fukui University assisted in meeting the publication costs of this article.

REFERENCES

1. A. Kitani, J. Izumi, Y. Hiromoto, and K. Sasaki, *Bull. Chem. Soc. Jpn.*, **57,** 2254 (1984).
2. A. G. MacDiarmid, L. S. Yang, W. S. Huang, and B. D. Humphery, *Synth. Met.*, **18,** 393 (1987).
3. L. Doubova, G. Mengoli, M. M. Musiani, and S. Valcher, *Electrochim. Acta,* **34,** 337 (1989).
4. J. C. Lacroix, K. K. Kanazawa, and A. Diaz, *This Journal,* **136,** 1308 (1989)
5. T. Kobayashi, H. Yoneyama, and H. Tamura, *J. Electroanal. Chem.*, **177,** 293 (1984).
6. Y. Shim, M. Won, and S. Park, *This Journal,* **137,** 538 (1990).
7. T. Osaka, S. Ogano, and K. Naoi, *ibid.*, **135,** 539 (1988); T. Osaka, S. Ogano, K. Naoi, and N. Oyama, *ibid.*, **136,** 306 (1989); T. Osaka, T. Nakajima, K. Naoi, and B. B. Owens, *ibid.*, **137,** 2139 (1990).
8. M. C. Miras, C. Barbero, R. Kotz, and O. Haas, *ibid.*, **138,** 335 (1991).
9. N. Kobayashi, K. Yamada, and R. Hirohashi, *Electrochim. Acta.*, **37,** 2101 (1992).
10. Z. Takehara, K. Kanamura, and S. Yonezawa, *ibid.*, **136,** 2767 (1989); K. Kanamura, S. Yonezawa, Y. Kawai, and Z. Takehara, *J. Electroanal. Chem.*, **301,** 291 (1991).
11. A. Volkov, G. Trourillon, R. C. Lacaze, and J. E. Dubois, *J. Electroanal. Chem. Interfacial Electrochem.*, **115,** 279 (1980).
12. T. Ohsaka, Y. Ohnuki, N. Oyama, G. Katagiri, and K. Kamisako, *ibid.*, **161,** 399 (1984).
13. W. Peukert, *Electrotech. Zeit.*, **18,** 287 (1897).
14. E. M. Genies, A. Boyle, M. Lapkowski, and C. Tsintavis, *Synth. Met.*, **36,** 139 (1990).
15. M. E. Jezefowicz, R. Laversanne, H. H. S. Javadi, A. J. Epstein, J. P. Pouget, X. Tang, and A. G. MacDiarmid, *Phys. Rev. B.*, **39,** 12958 (1989).
16. M. Laridjani and J. P. Pouget, E. M. Scherr and A. G. MacDiarmid, M. E. Jezefowicz, and A. J. Epstein, *Macromolecules,* **25,** 4106 (1992).
17. P. Walden, H. Ulich and G. Busch, *Z. Physik. Chem.*, **A123,** 429 (1926); P. Walden and E. J. Birr, *ibid.*, **A153,** 1 (1931).

Surface Effects in the Hydrogen Evolution Reaction on Ni-Zn Alloy Electrodes in Alkaline Solutions

A. C. D. Angelo*,[a] and A. Lasia*

Départment de chimie, Université de Sherbrooke, Sherbrooke, Québec, Canada J1K 2R1

ABSTRACT

Hydrogen evolution reaction was studied on Ni-Zn (25% of Ni before leaching) in 1 *M* NaOH at 25°C. These electrodes were characterized by very low Tafel slopes of 67 mV dec^{-1}. Other techniques used included potential and current pulse, potential relaxation in an open circuit, and ac impedance spectroscopy. Analysis of the experimental results led to the conclusion that hydrogen adsorption in the surface layers was responsible for the observed behavior. Influence of the oxidation of the electrode surface and the addition of poisons, thiourea and cyanides, were also studied. These processes inhibit the hydrogen absorption and restore "normal" Tafel slopes. Kinetic parameters of the hydrogen evolution reaction were determined.

Introduction

Hydrogen is one of the most promising energy carriers an alternative to fossil fuels.[1,2] Gaseous hydrogen can be easily produced by water electrolysis and further used as a nonpolluting fuel directly in the internal combustion engines or reconverted to electricity in fuel cells. The hydrogen evolution reaction (HER) has been studied on various electrode materials in order to find better electrocatalysts and to understand better the kinetics and mechanism of this process.[3-11] Between the best electrode material for the HER are Raney-type alloys.[12-31] They consist of an electrocatalytically active metal, *e.g.*, Ni or Co, and the other more active one, *e.g.*, Al or Zn, which can be easily leached out in alkaline solutions leaving a large active surface area. These materials are well known in the catalytic hydrogenation of organic compounds. In our earlier papers we have studied the HER on various Raney Ni-Al [17,20,26,28-31] and Ni-Zn electrodes.[19,21] Ni-Al alloys usually are characterized by nonlinear Tafel plots, their slopes increase with overpotential, while Ni-Zn alloys are characterized by low Tafel slopes, which are usually linear and increase with the increase in nickel content.[19] The morphological surface studies show formation of a "dry-mud"-type structure[19] because the alloy shrinks upon leaching.[24] During the leaching process a small amount of large pores and a large amount of very narrow pores are formed, especially for Zn-rich alloys.[19,24,25] The leaching process is usually not complete and a small amount of Zn stays in the alloy and may leach out slowly with time.[22,25,32] Tafel slopes obtained on Ni-Zn electrodes are in the range 55 to 90 mV dec^{-1} depending on Zn content.[19] They cannot be explained by the Volmer-Heyrovsky-Tafel reaction mechanism with the transfer coefficient

* Electrochemical Society Active Member.
[a] Permanent address: Departamento de Quimica, UNESP, Bauru, SP, Brazil.

close to 0.5. This mechanism predicts the possibility of obtaining slopes of 30 or 40 mV dec^{-1} at low overpotentials which should become 118 (or ∞) at more negative potentials. Nonlinear slopes may be observed in the intermediate range. To explain these slopes in terms of the Volmer-Heyrovsky reaction mechanism one should assume very large values of transfer coefficients,[19] which are not very probable in terms of the current charge-transfer theories. De Giz *et al.*[33] tried to explain these slopes assuming the Volmer-Heyrovsky-Tafel reaction mechanism (rate of Tafel reaction was negligible). They reproduced low Tafel slopes at low overpotentials, below 0.1 V. These intermediate slopes are possible at these overpotentials. However, the rate constants presented by de Giz *et al.* produce a "normal" slope of 120 mV dec^{-1} at the overpotentials larger than 0.1 V, and they cannot explain the observed experimental behavior. In fact, it is clearly visible from Fig. 5 in Ref. 33 that the calculated Tafel slope increases with overpotential while the experimental one stays small and constant. Our studies showed[19] that the slopes are linear in the overpotential range studied, *i.e.*, from −0.18 to −0.3 V, depending on the electrode composition.

The purpose of the present paper is to better understand the mechanism of the HER on electrodeposited Ni-Zn electrodes. Various steady-state and relaxation techniques were used and the electrode surface was modified by oxidation and adsorption of neutral and ionic species.

Experimental

Ni-Zn electrodes were prepared by electrodeposition as described earlier.[19] Their composition was verified by the inductively coupled plasma (ICP) technique (ARI FISONS 3506 AES) after dissolution in nitric acid. It was found that they contained 25% in Ni. Before electrochemical studies zinc was leached out in alkaline solution.[19]

The steady-state polarization, chronoamperometric, and chronopotentiometric experiments were carried out using EG&G Model 273A potentiostat controlled by an IBM-PC compatible microcomputer. AC impedance data were obtained using EG&G Model 5206 lock-in analyzer for the measurements between 10 kHz and 5 Hz and a fast Fourier transform (FFT) technique for frequencies between 5 and 0.05 Hz. Data acquisition for the open-circuit potential decay (OCPD) experiments was carried out using Model PRO-92 Nicolet digital oscilloscope.

All the electrochemical experiments were carried out at 25°C in 1 *M* NaOH (BDH-Aristar 99.99%) solution using deionized water (Barnstead-Nanopure). Nitrogen was bubbled through the solution before and during the experiments. A high surface area Ni foil was used as a counter-electrode and Hg/HgO/1 *M* NaOH as a reference electrode. Both electrodes were separated from the working electrode compartment by a fritted glass. Thiourea (Anachemia) and sodium cyanide (Anachemia) were used without further purification.

Results

Sodium hydroxide solutions.—In order to explain the nature of low values of Tafel slopes they were measured in two different experiments. The first one consisted of the application of a constant current of 127 mA cm^{-2} for 15 min followed by the application of various currents down to 0.03 μA cm^{-2} for 5 s and recording the electrode potential at each current value. The whole procedure was repeated until reproducible Tafel curves were obtained. The second method consisted of keeping the electrode at an open-circuit potential (OCP) for 30 min and then the application of a potential pulse and measuring the current as soon as the first stable value was obtained, that is about 0.5 s after application of the pulse. Then the electrode was kept at the open-circuit potential again, and the whole procedure was repeated at another potential. At lower overpotentials (<110 mV) the current was increasing with time to a steady-state plateau. At higher overpotentials first a small plateau was formed and then the current increased to form another plateau. Figure 1 shows an example of such chronoamperometric curve. In this case the first plateau was used in constructing Tafel plots. Figure 2 shows two Tafel plots obtained using these two methods and the corresponding Tafel parameters are presented in Table I.

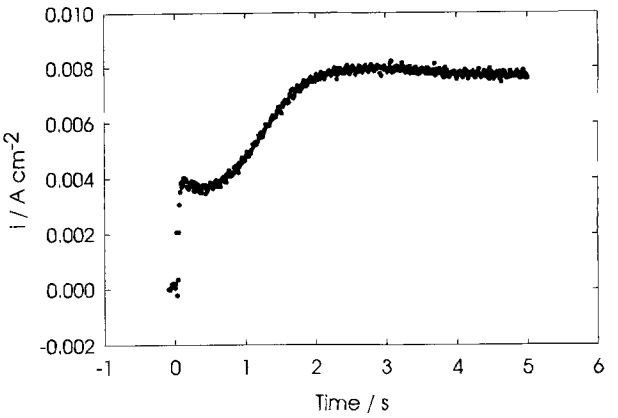

Fig. 1. Chronoamperometric transients obtained on Ni-Zn electrode in 1 *M* NaOH at 25°C, potential pulse from η = 0 to −0.198 V.

The Tafel slope obtained in the steady-state experiments, b = 67 mV dec^{-1}, was much lower than the theoretical value of 118 mV dec^{-1} predicted for the Volmer-Heyrovsky mechanism with β = 0.5. As was mentioned above such a small slope cannot be explained in terms of the Volmer-Heyrovsky-Tafel mechanism. Moreover, these slopes cannot be explained in terms of fractal or porous electrode models, which predict increase (or doubling) of Tafel slopes.[34,35] On the other hand the Tafel slope obtained in the potential pulse experiments, b = 109 mV dec^{-1}, was close to the theoretical one. In order to better understand the observed behavior series of other experiments were performed.

In the subsequent experiment the effect of polarization time on the galvanostatically recorded steady-state Tafel curves was studied. In these experiments the electrode potential was measured after 1 to 60 s after application of a constant current. The obtained Tafel curves are displayed in Fig. 3. There was no change in the Tafel plots at negative overpotentials but the anodic shift of the open-circuit potential was observed at longer polarization times, that is, at low cathodic currents the potential was more positive than the thermodynamic value of the HER. This result indicated that other reactions then the HER determined the kinetics of the process at these potentials. These could be, for example, corrosion of residual quantities of zinc inside the pores left out after the leaching process.

Chronopotentiometric transients obtained (*i*) after keeping the electrode at an open-circuit potential for 4 h and (*ii*) after polarization for 24 h at 100 mA cm^{-2}, are shown in Fig. 4. It is evident that when the electrode was previously polarized at high current density, the potential stabilized very quickly and that kept the open-circuit potential relaxed much more slowly. This experiment indicates that some changes at the electrode surface take place during the polarization.

Behavior of these electrodes was also studied using ac impedance spectroscopy. As it was shown earlier[36] the faradaic admittance, Y_f, of the HER is described as

$$Y_f = A + B/(j\omega + C) \quad [1]$$

Table I. Tafel parameters obtained from the steady-state galvanostatic and potential pulse experiments of the HER on Ni-Zn (25% of Ni before leaching) in 1 *M* NaOH at 25°C.

Technique	b (mV dec^{-1})	$i_o \cdot 10^4$ (A cm^{-2})	$-\eta_{250}$ (mV [a])
Steady state	67	0.13	288
Potential pulse	109	18.8	231

[a] $-\eta_{250}$ is the overpotential at a current density of 250 mA cm^{-2}.

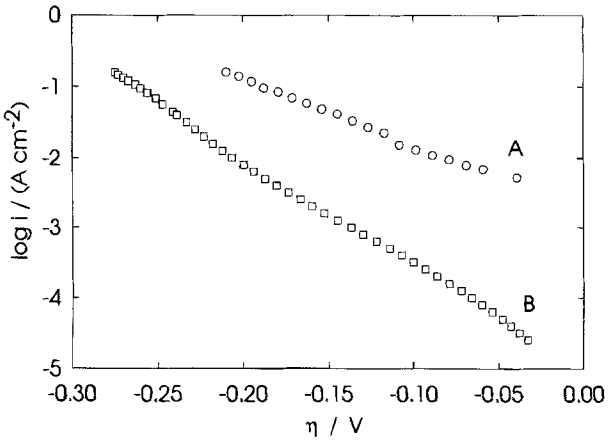

Fig. 2. Tafel curves obtained from (A) potentiostatic pulse and (B) steady-state experiments in 1 *M* NaOH at 25°C.

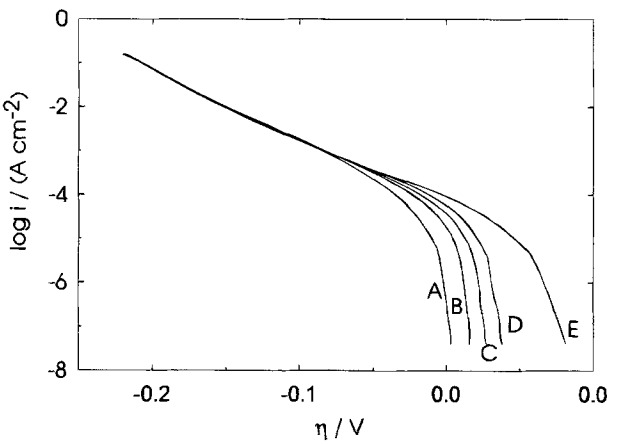

Fig. 3. Influence of time of application of constant current on steady-state Tafel curves; measurements after A, 1; B, 5; C, 10; D, 30; and E, 60 s.

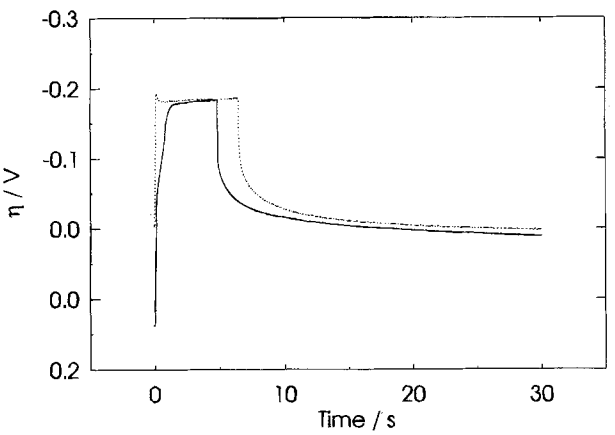

Fig. 4. Chronopotentiometric transients obtained on the electrode kept for 4 h at open-circuit potential (continuous line) and polarized at 100 mA cm^{-2} for 24 h (dotted line).

where

$$A = -F(\partial r_0/\partial\eta)_\Theta \quad [2]$$

$$B = -(F^2/\sigma_1)(\partial r_0/\partial\Theta)_\eta(\partial r_1/\partial\eta)_\Theta \quad [3]$$

$$C = -(F/\sigma_1)(\partial r_1/\partial\Theta)_\eta \quad [4]$$

$r_0 = v_1 + v_2$, $r_1 = v_1 - v_2 - 2v_3$, v_1, v_2, and v_3 are the rates of the Volmer, Heyrovsky, and Tafel reactions, respectively, and σ_1 is the charge necessary for a monolayer coverage by atomic hydrogen. The equivalent circuit consists of the solution resistance in series with the parallel connection of the CPE element and faradaic impedance.[10,11] This model predicts either two semicircles or a semicircle followed by an inductive loop.[36,37-39]

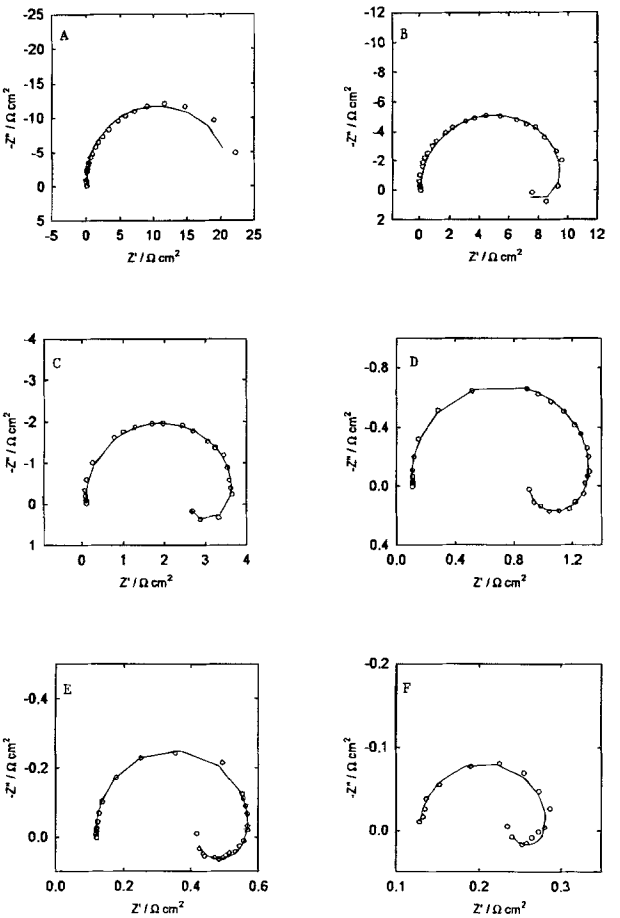

Fig. 5. Complex plane plots obtained on Ni-Zn electrode in 1 *M* NaOH; η = (A) −0.148, (B) −0.168, (C) −0.188, (D) −0.208, (E) −0.228, and (F) −0.268 V.

Figure 5 shows complex plane plots obtained for the HER at different overpotentials. At overpotentials higher than −0.15 V an inductive loop appeared in a low frequency range. In our earlier studies[19] this loop was not reported because the ac impedance results were studied at higher frequencies (the lower frequency limit was around 1 Hz for overpotentials more negative than −0.15 V). Although such an inductive loop is theoretically possible, it is quite unusual for the HER and it has only been found for by Searson[40] for hydrogen absorbing palladium electrodes in alkaline solutions. De Giz *et al.*[33] observed one semicircle at 25°C on Ni-Zn electrodes and two semicircles at higher temperatures. They attributed this fact to the changes of hydrogen adsorption with temperature.

The experimental ac impedance curves were analyzed using a complex nonlinear least squares (CNLS)[38] program in order to determine the parameters *A*, *B*, and *C* of the faradaic process as well as the CPE parameters. The values

Table II. Parameters A, B, and C determined for the HER on Ni-Zn electrode in 1 *M* NaOH at 25°C.

−η (V)	*A* (Ω^{-1} cm^{-2})	*B* (Ω^{-1} cm^{-2} s^{-1})	*C* (s^{-1})
0.068	0.00101	—	—
0.108	0.0216	—	—
0.148	0.0742	0.0138	0.0476
0.168	0.164	0.0486	0.755
0.188	0.397	0.245	1.28
0.208	0.992	1.08	1.79
0.228	2.32	3.70	2.56
0.248	4.35	8.58	3.09
0.268	6.78	13.75	4.29

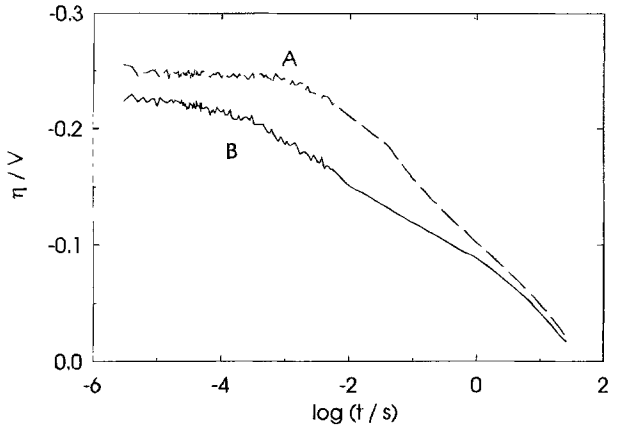

Fig. 6. Open-circuit relaxation curves obtained for the Ni-Zn electrode: A, after long time polarization and, B, for the electrode kept at the open-circuit potential.

of parameters *A*, *B*, and *C* are displayed in Table II. They could be, in general, used to estimate the rate constants[10,11,19] of the HER. However, it was impossible to fit these parameters, together with the steady-state polarization data, to the HER mechanism. Subsequently, we have simulated values of *A*, *B*, and *C* parameters for the Volmer-Heyrovsky and Volmer-Heyrovsky-Tafel reaction mechanisms using various values the rate constants k_1, k_{-1}, k_2, and k_3 between 10^{-3} and 10^{-13} mol cm^{-2} s^{-1}. Again, it was impossible to obtain values of parameters *A*, *B*, and *C* close to the experimental ones at these overpotentials. Therefore, it is evident that the Volmer-Heyrovsky-Tafel mechanism cannot explain the observed ac impedance experimental behavior.

Potential relaxation in an open circuit was also used to study the electrode behavior. Possibilities of this technique for hydrogen adsorption was discussed earlier.[11,20,41,42] Figure 6 shows the open-circuit potential decay (OCPD) curves for a freshly prepared electrode and the same electrode after polarization at the potentials corresponding to the hydrogen evolution. The electrode, which was polarized at a constant current for a long time, relaxed more slowly than that kept at the open-circuit potential before application of the current pulse. Even after long times (>60 s) the potential did not reach the equilibrium value.

It is well known[10,17] that oxidation of the electrode surface increases activity toward the HER. In our earlier studies on oxidized polycrystalline Ni electrodes such an increase in activity was connected with appearance of two Tafel slopes.[10] Besides, noble metal oxides were found to be good catalysts for the HER. [8] In our experiments the electrodes were cycled between −1.1 and 0.7 V *vs.* Hg/HgO/NaOH electrode, *i.e.*, until Ni(III) oxide was formed on the

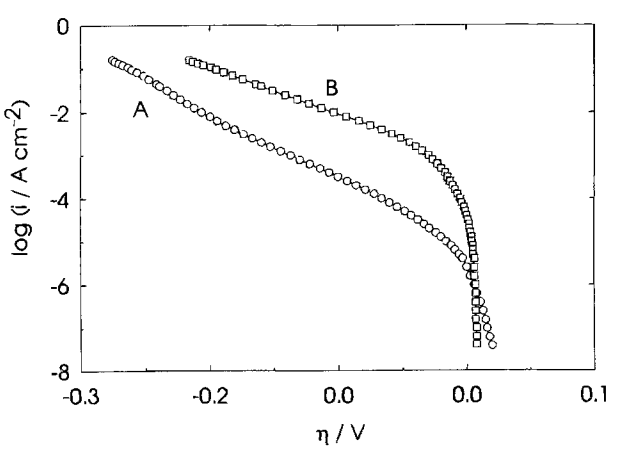

Fig. 7. Tafel plots obtained on Ni-Zn electrode, A, and after cycling to positive potentials, B; see text for details.

Table III. Tafel parameters for the HER on Ni-Zn electrode in 1 *M* NaOH at 25°C before and after oxidation-reduction cycling (see text for details).

Conditions	b (mV dec^{-1})	$i_o \cdot 10^4$ (A cm^{-2})	$-\eta_{250}$ (mV)
No cycling	70	0.66	251
After cycling	97	8.5	239

electrode surface. Figure 7 presents Tafel curves obtained before and after ten such cycles. An increase of the electrode activity and also an increase of the Tafel slope was observed. That increased activity was maintained up to 20 h under cathodic polarization. The corresponding Tafel parameters are presented in Table III.

The activity of oxidized electrodes was also studied using ac impedance spectroscopy. Figure 8 shows corresponding complex plane plots. They are very different from those for nonoxidized surfaces, Fig. 5. The inductive loop present in Fig. 5 disappeared and two semicircles were obtained at lower overpotentials and only one deformed semicircle at higher ones. The first semicircle was almost overpotential independent while the second one decreased continuously with the increase of overpotential until it vanished. Additionally, at higher overpotentials, a linear segment of the complex plane plot was found in a high frequency range, which is characteristic of porous electrodes.[34,43] Very similar results were reported earlier on Ni-Zn [44] and Ni-Al [28] pressed powder electrodes in 1 *M* NaOH, where it was suggested that the first semicircle was related to electrode porosity.[45]

Influence of poisons.—In order to better understand electrode behavior, surface active poisons were added to the solution. Two model compounds were chosen: one neutral, thiourea, and one ionic, cyanide. Figures 9 and 10

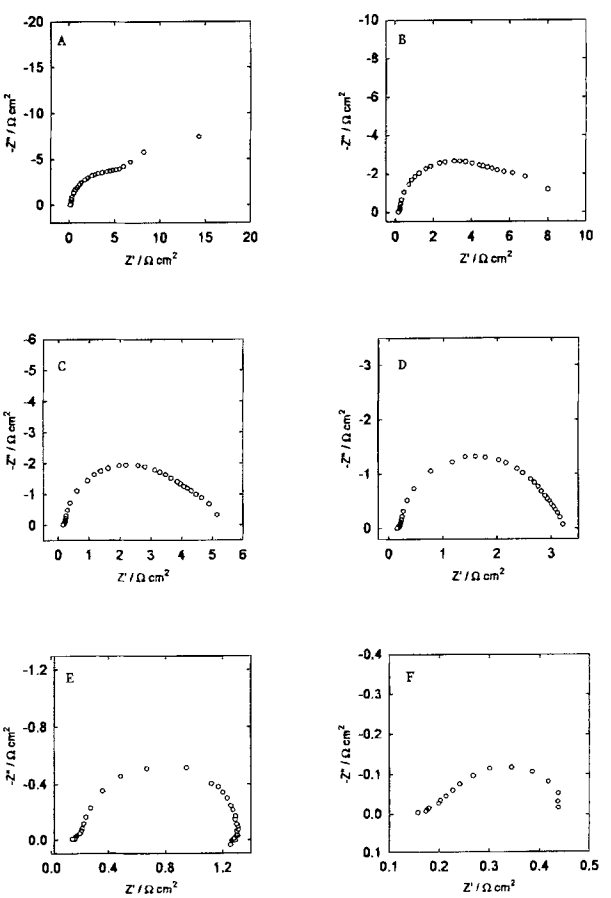

Fig. 8. Complex plane plots for oxidized (cycled) Ni-Zn electrode; η = (A) −0.028, (B) −0.068, (C) −0.088, (D) −0.108, (E) −0.148, and (F) −0.228 V.

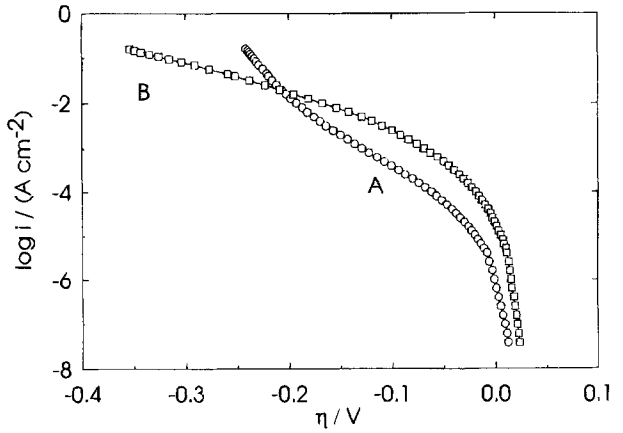

Fig. 9. Tafel curves obtained on Ni-Zn electrode in 1 *M* NaOH (A) and after adding 25 m*M* of thiourea (B).

show examples of Tafel plots for the HER in the presence of these compounds and the corresponding Tafel parameters are displayed in Table IV. These results indicate that in both cases slopes close to the theoretical value for the Volmer-Heyrovsky reaction mechanism (118 mV dec^{-1}) were obtained. In the presence of thiourea an increase in electrode activity at lower overpotentials was observed while the addition of cyanides caused decrease in activity. An increase in Tafel slopes and a decrease in activity was also observed earlier on Ni-Zn electrodes after the addition of pyridine to the solution.[21]

AC impedance spectra obtained in 1 *M* NaOH in the presence of 25 m*M* thiourea and 0.5 m*M* CN^- are displayed in Fig. 11 and 12. Only one semicircle was observed at all overpotentials, contrary to the results in pure NaOH solution. Further increase in the concentration of thiourea up to 0.1 *M* had no significative effect on the Tafel or impedance plots.

The experimental steady-state currents and charge-transfer resistances a functions of overpotential were used to estimate the rate constants of the HER. It was sufficient to suppose the Volmer-Heyrovsky mechanism to explain the reaction mechanism. The experimental and fitted Tafel curves and parameters *A* (inverse of the charge-transfer resistance) are shown Fig. 13. The estimated rate constants are $k_1 = (3.16 \pm 0.4) \cdot 10^{-8}$; $k_{-1} = (3.78 \pm 0.2) \cdot 10^{-10}$, and $k_2 = (3.16 \pm 0.08) \cdot 10^{-9}$ mol cm^{-2} s^{-1} in the presence of thiourea. For the HER in the absence of the adsorbing species similar values were obtained earlier $k_1 = (1.2 \pm 0.6) \cdot 10^{-7}$ and $k_2 = (1.6 \pm 0.1) \cdot 10^{-9}$ mol cm^{-2} s^{-1}, however, these electrodes are characterized by quite different transfer coefficients.

In the presence of CN^- only one value, the rate constant $k_2 = (6.4 \pm 3.1) \cdot 10^{-11}$ mol cm^{-2} s^{-1}, could be estimated; the

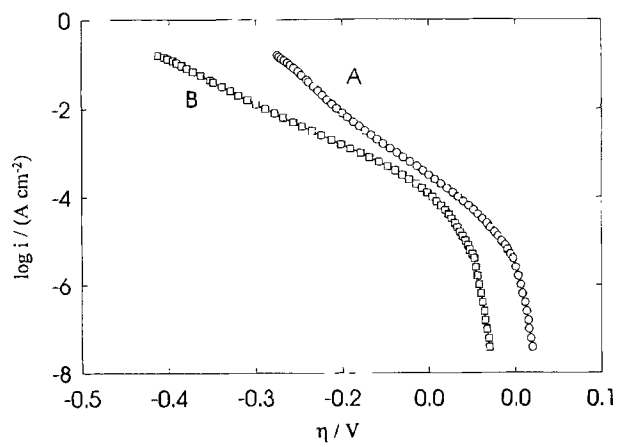

Fig. 10. Tafel plots obtained on Ni-Zn electrode in 1 *M* NaOH (A) and after adding 0.5 m*M* of CN^- (B).

Table IV. Tafel parameters obtained for the HER in the presence of poisons in 1 M NaOH at 25°C.

Solution	b (mV dec^{-1})	$i_o \cdot 10^4$ (A cm^{-2})	$-\eta_{250}$ (V)
1 *M* NaOH	67	0.13	288
+25 m*M* thiourea	115	3.0	337
+0.5 m*M* CN^-	101	0.48	377

values of other rate constants were much larger than k_2 and their errors were larger than their values. Although, in general, two equivalent solutions exist for the Volmer-Heyrovsky mechanism in which values of $k_1 \leftrightarrow k_2$ and $k_{-1} \leftrightarrow k_{-2}$ and $\beta_1 \leftrightarrow \beta_2$ are interchanged[10,11] it was supposed here that the kinetics of the Heyrovsky reaction is rate limiting, that is the surface coverage increases with negative overpotential.

Figure 14 presents the dependence of the double-layer capacitances, C_{dl}, as a function of the overpotential, obtained using model described by Brug *et al.*[46] In the presence of cyanides and thiourea, C_{dl} is practically overpotential independent, but in pure NaOH solutions C_{dl} changes nonlinearly with overpotential, the largest changes occur at low overpotentials. C_{dl} values for CN^- solutions are the lowest indicating strong adsorption. On the other hand, double-layer capacitances in the presence of thiourea are the largest and, at more negative overpotentials, they are the same as those found for the pure NaOH solutions, indicating that there is no change in the apparent surface area.

Discussion

Our studies of the HER on electrodeposited Ni-Zn electrodes, after leaching out Zn, have shown that the reaction mechanism in pure NaOH solutions is different than that on the oxidized surface or in the presence of thiourea or

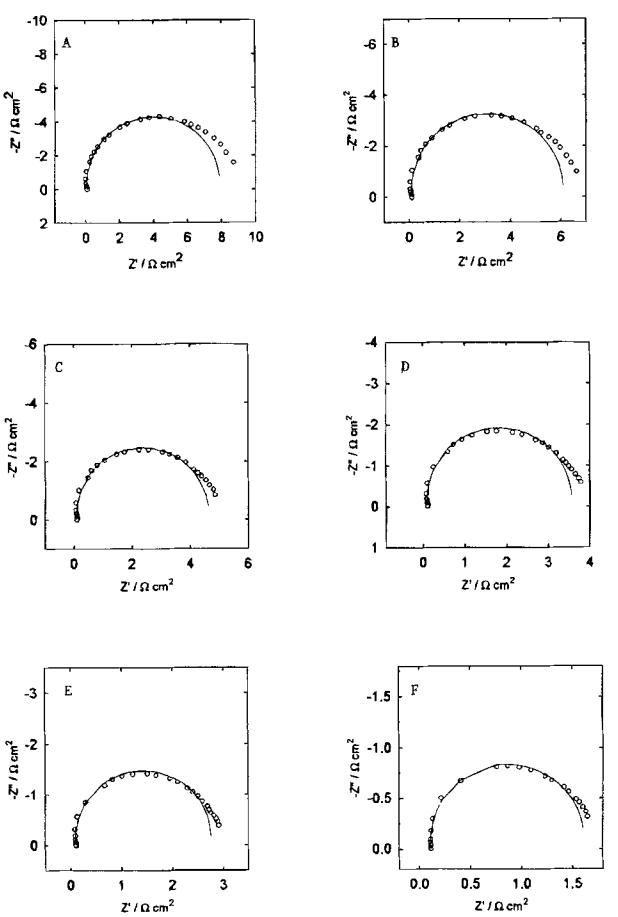

Fig. 11. Complex plane plots on Ni-Zn electrode in 1 M NaOH containing 25 mM of thiourea; η = (A) −0.148, (B) −0.168, (C) −0.188, (D) −0.208, (E) −0.228, and (F) −0.268 V.

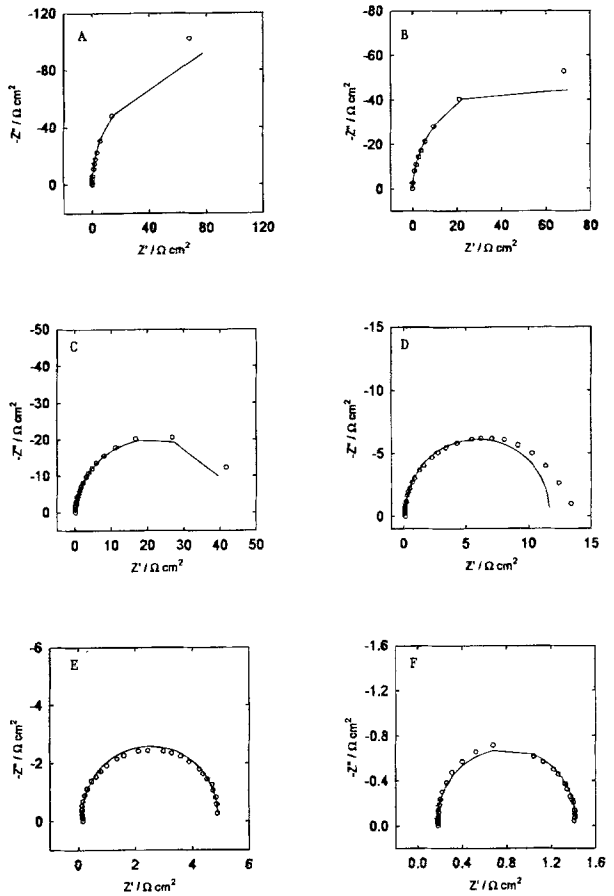

Fig. 12. Complex plane plots on Ni-Zn electrode in 1 *M* NaOH and 0.5 mM of CN^-; η = (A) −0.148, (B) −0.188, (C) −0.228, (D) −0.268, (E) −0.298, and (F) −0.338 V.

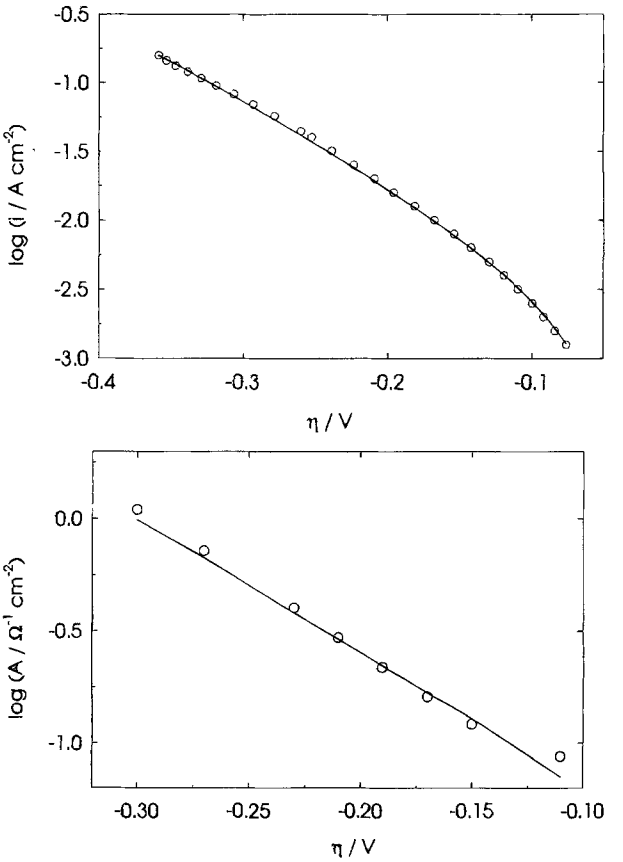

Fig. 13. Tafel plot (A, top) and dependence of log A (B, bottom) as a function of overpotential on Ni-Zn electrode in 1 *M* NaOH and 25 mM of thiourea.

cyanides. The electrodes at which the HER was carried out for a long time behave differently from the electrodes kept at the open-circuit potential. Tafel slopes determined on polarized electrodes were smaller than those determined on the electrodes kept at the equilibrium potential.

In the chronopotentiometric experiments the measured potential increased more slowly when the current pulse was applied to the electrode kept at the OCP, and it increased very fast when applied to the electrode previously polarized at the negative potentials. Besides, the OCPD curves decreased faster for the electrode kept at the OCP.

The ac impedance spectra showed an inductive loop at more negative overpotentials. Although that loop is predicted for the HER [36,37,39] the parameters obtained could not be explained in terms of the Volmer-Heyrovsky-Tafel mechanism. Oxidation of the electrode surfaced led to an increase in the Tafel slope although it was still lower than that predicted for the HER.

The experimental results presented above suggested that the hydrogen absorption into metal (or at least in the surface layer), occurring at long polarization times, could be responsible for the observed behavior. The electrode kept at the open-circuit potential did not contain any hydride and displayed a "normal" behavior. Initial current, measured after the application of the potential pulse, led to the Tafel slope of 109 mV dec^{-1} and after longer polarization the current increased. Recently, Machado *et al.* [47] found similar effects for Ni-Zn and Ni-Co-Zn electrodes using measurements of Tafel slopes 4 ms after the application of the current pulse, however, they did not present any transient curves. From the studies presented above, it follows that the stabilization of the electrode potential depends on the experimental current density (potential), and the measurements should be taken only after reaching a plateau. Machado *et al.* [47] attributed the observed behavior to the formation of the subsurface hydride. Besides, Machado and Avaca [48] suggested formation of the hydride for the HER on Ni electrode in alkaline solutions. It should be mentioned, however, that loss of activity is often attributed to the surface hydride formation [49,50] although hydrogen absorbing materials as $LaNi_5$ are very good catalysts for the HER. [32] Divisek *et al.* [32] also suggested that one should consider two surface species present during the HER: hydrogen absorbed on the surface and the top layer of absorbed hydrogen which should be treated as a separate species. However this hypothesis has not been confirmed experimentally yet.

Other effects were also proposed to explain small Tafel slopes observed on certain active materials. Rausch and Wendt [24] found that the high concentration polarization of hydrogen in pores would lead to lower Tafel slopes of 80 to 110 mV dec^{-1}. Similarly, Losev *et al.* [51] suggested a Nerstian Tafel slope (2.3 *RT*/nF) and Müller and Heidrich [52] even smaller slopes of 15 mV dec^{-1} for gas evolving electrodes.

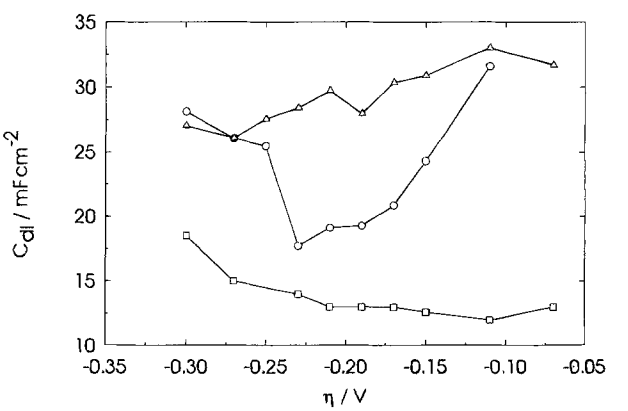

Fig. 14. Double-layer capacitances determined from ac impedances in 1 *M* NaOH (○), and with 25 mM thiourea (△) and with 0.5 mM CN^- (□).

However, this behavior should lead to a change of the slope with overpotential which was not observed in our case, where Tafel plots were linear in a large potential range.[19] Besides, it is not clear why such large changes in slopes should be observed after the adsorption of thiourea or cyanides; adsorption should not influence the hydrogen mass-transfer process because the surface morphology was not affected by these processes and the double-layer capacitances do not show any important changes in the real surface area.

The proposed hydride formation in the porous nickel layer close to the electrode surface could change the Ni surface properties with overpotential and affects the reaction kinetics and mechanism leading to smaller Tafel slopes and different ac behavior. Surface oxidation or adsorption of neutral or ionic substance inhibits the hydride formation process and restores the typical behavior found for other electrodes. Adsorption of thiourea increases the electrode activity at low overpotentials in relation to the possible Ni-S formation, known to enhance the kinetics of the HER.[53-57] This effect is different from the poisoning effect observed on noble metals. In fact, thiourea was added to the nickel plating solution[53,55] to obtain Ni-S alloy. On the other hand, adsorption of cyanides poisons the electrode and decreases its activity toward the HER.

It was reported earlier[22,25,58] that residual zinc content in the electrode is important for the electrode catalytic activity. In our studies we have used thin alloy layers (10 to 15 μm) deposited on small electrodes (0.32 cm^2), and the residual concentration of zinc in the solution was negligible. These studies were carried out after long time polarization, and the changes in zinc content in the electrode during the registration of curves were negligible.

Acknowledgments

The postdoctoral fellowship for A. C. D. Angelo from the Fundaçao de Amparo a Pesquisa do Estado de São Paulo (FAPESP-Brazil), and the FCAR and NSERC funding are gratefully acknowledged.

Manuscript received Nov. 28, 1994; revised manuscript received June 13, 1995.

Université de Sherbrooke assisted in meeting the publication costs of this article.

REFERENCES

1. G. P. Dinga, *Int. J. Hydrogen Energy,* **14,** 777 (1989).
2. T. N. Veziroglu and F. Barbir, *ibid.,* **17,** 391 (1992).
3. M. Enyo, in *Comprehensive Treatise of Electrochemistry,* Vol. 7, J. O'M. Bockris, E. Yeager, S. U. M. Khan, and R. E. White, Editors, p. 241, Plenum Press, New York (1983).
4. B. V. Tilak, A. C. Ramamurthy, and B. E. Conway, *Proc. Indian Acad. Sci. (Chem. Sci.),* **97,** 359 (1986).
5. B. E. Conway, *Sci. Prog. Oxford,* **71,** 479 (1987).
6. J. O'M. Bockris, in *Comprehensive Treatise of Electrochemistry,* Vol. 3, B. E. Conway, E. Yeager, and R. E. White, Editors, Plenum Press, New York (1981).
7. *Electrochemical Hydrogen Technologies,* H. Wendt, Editor, Elsevier, New York (1990).
8. S. Trasatti, in *Advances in Electrochemical Science and Engineering,* Vol. 2, H. Grischer and C. W. Tobias, Editors, p. 1, VCH, New York (1992).
9. E. R. Gonzalez, G. Tremiliosi-Filho, and M. J. de Giz, in *Current Topics in Electrochemistry,* **2,** 167 (1993).
10. A. Lasia and A. Rami, *J. Electroanal. Chem.,* **294,** 123 (1990).
11. A. Lasia, in *Current Topics in Electrochemistry,* **2,** 239 (1993).
12. B. E. Conway, H. Angerstein-Kozlowska, and M. A. Sattar, *This Journal,* **130,** 1825 (1983).
13. L. Lohrberg and P. Kohl, *Electrochim. Acta,* **29,** 1557 (1984).
14. E. Endoh, H. Otouma, and Y. Oda, *Int. J. Hydrogen Energy,* **12,** 473 (1987).
15. T. Kenjo, *Electrochim. Acta,* **33,** 41 (1988).
16. J. Divisek, P. Malinowski, J. Mergel, and H. Schmitz, *Int. J. Hydrogen Energy,* **13,** 141 (1988).
17. Y. Choquette, L. Brossard, A. Lasia, and H. Ménard, *This Journal,* **137,** 1723 (1990); *Electrochim. Acta,* **35,** 1251 (1990).
18. J. Divisek, J. Mergel, and H. Schmitz, *Int. J. Hydrogen Energy,* **15,** 105 (1990).
19. L. Chen and A. Lasia, *This Journal,* **138,** 3321 (1991).
20. A. Rami and A. Lasia, *J. Appl Electrochem.,* **22,** 376 (1992).
21. L. Chen and A. Lasia, *This Journal,* **139,** 1058 (1992).
22. J. Balej, J. Divisek, H. Schmitz, and J. Mergel, *J. Appl. Electrochem.,* **22,** 711 (1992).
23. M. J. De Giz, S. A. S. Machado, L. A. Avaca, and E. R. Gonzalez, *ibid.,* **22,** 973 (1992).
24. S. Rausch and H. Wendt, *ibid.,* **22,** 1025 (1992).
25. T. Borucinski, S. Rausch, and H. Wendt, *ibid.,* **22,** 1031 (1992).
26. P. Los, A. Rami, and A. Lasia, *ibid.,* **23,** 135 (1993).
27. M. Okido, J. K. Depo, and G. A. Capuano, *This Journal,* **140,** 127 (1993).
28. L. Chen and A. Lasia, *ibid.,* **140,** 2474 (1993).
29. A. Kam Cheong, A. Lasia, and J. Lessard, *ibid.,* **140,** 2721 (1993).
30. A. Kam Cheong, A. Lasia, and J. Lessard, *ibid.,* **141,** 975 (1994).
31. D. Miousse, V. Borck, and A. Lasia, *J. Appl. Electrochem.,* **25** (1995).
32. J. Divisek, H. Schmitz, and B. Steffen, *Electrochim. Acta,* **39,** 1723 (1994).
33. M. J. De Giz, G. Tremiliosi-Filho, and E. R. Gonzalez, *ibid.,* **39,** 1775 (1994).
34. R. de Levie, in *Advances in Electrochemistry and Electrochemical Engineering,* Vol. 6, P. Delahay and C. W. Tobias, Editors, p. 239, Wiley, New York (1967).
35. W. H. Mulder and J. H. Sluyters, *J. Electroanal. Chem.,* **282,** 27 (1990).
36. D. A. Harrington and B. E. Conway, *Electrochim. Acta,* **12,** 1712 (1987).
37. C.-N. Cao, *ibid.,* **35,** 831 (1990).
38. J. R. Macdonald, *Impedance Spectroscopy,* Wiley, New York (1987).
39. J.-P. Diard, B. Le Gorrec, and C. Montella, *J. Electroanal. Chem.,* **326,** 13 (1992).
40. P. C. Searson, *Acta Metall. Mater.,* **39,** 2519 (1991).
41. D. A. Harrington and B. E. Conway, *J. Electroanal. Chem.,* **221,** 1 (1987).
42. L. Bai, *ibid.,* **355,** 37 (1993).
43. P. Los, A. Lasia, L. Brossard, and H. Ménard, *ibid.,* **360,** 101 (1993).
44. L. Chen and A. Lasia, *This Journal,* **139,** 3214 (1992).
45. H. Kreiser, K. D. Beccu, and M. A. Gutjahr, *Electrochim. Acta,* **21,** 539 (1976).
46. G. J. Brug, A. L. B. van der Eeden, M. Sluyters-Rehbach, and J. H. Sluyters, *J. Electroanal. Chem.,* **176,** 275 (1984).
47. S. A. S. Machado, J. Tiengo, P. De Lima Neto, and L. A. Avaca, *Electrochim. Acta,* **39,** 1757 (1994).
48. S. A. S. Machado and L. A. Avaca, *ibid.,* **39,** 1385 (1994).
49. D. M. Soares, O. Teschke, and I. Torriani, *This Journal,* **139,** 98 (1992).
50. D. M. Soares, M. U. Kleinke, I. Toriani, and O. Teschke, *Int. J. Hydrogen Energy,* **19,** 573 (1994).
51. V. V. Losev, N. Ya. Buné, and L. E. Chuvayeva, *Electrochim. Acta,* **34,** 929 (1989).
52. L. Müller and H.-J. Heidrich, *Sov. Electrochem.,* **25,** 1027 (1989).
53. H. Vandenborne, Ph. Vermeiren, and R. Leysen, *Electrochim. Acta,* **29,** 297 (1984).
54. Yu. I. Kryulov, S. F. Chernyshov, A. G. Pshenichnikov, L. I. Al'tentaller, I. P. Naumov, Ya.S. Lapin, and N. P. Kuznetsova, *Sov. Electrochem.,* **29,** 640 (1991).
55. I. Paseka, *Electrochim. Acta,* **38,** 2449 (1993).
56. E. R. Gonzalez, L. A. Avaca, G. Tremiliosi-Filho, S. A. S. Machado, and M. Ferreira, *Int. J. Hydrogen Energy,* **19,** 17 (1994).
57. H. Wendt, *Electrochim. Acta,* **39,** 1749 (1994).
58. J. Divisek, J. Mergel, and H. Schmitz, *Int. J. Hydrogen Energy,* **15,** 105 (1990).